SUPPLEMENTAL METHODS

Isolation of canine adipose stromal cells and skin fibroblasts. The animal protocol was approved by the Stanford Animal Research Committee. Three one-year old Mongrel dogs (Marshall Farm, CA) were anesthetized with 5 mg/kg tiletamine/zolazepam (Webster, Sterling, MA) and were placed prone on the operating table with sterile preparation of the posterior dorsal region. To obtain canine fibroblasts (cFibro), an elliptical skin incision was performed on dorsal surface of these dogs. This incision was carried through the dermis and into the underlying adipose tissue. This ellipse was then sharply resected and underlying hemostasis was obtained. Once the ellipse was removed, the adipose and tissue underlying the dermis was meticulously removed. The ellipse was closed primarily with a layered closure with deep 2-0 vicryl and superficial 2-0 nylon sutures. Subsequently, the dermal and epidermal layers were taken to the laboratory and fibroblast harvest was performed using collagenase II digestion at 37^{o}C overnight. The adipose tissue from dogs was resected sharply and separated from the overlying skin. Adipose specimens were digested with collagenase II at 37^{o}C for 4 hours. The stromal vascular fraction was then pelleted, filtered at 100 micron pore size, and primary cultures of canine adipose stromal cells (cASCs) established at 37^{o}C and 5% CO_2.

Cell culture and maintenance. cASCs were maintained with Dulbecco's Modified Eagle Medium (DMEM) (Invitrogen, Carlsbad, CA) containing 10% fetal bovine serum (FBS) (Invitrogen), Glutamax-I (Invitrogen), 4.5 g/L glucose (Sigma, St. Louis, MO), 110 mg/L sodium pyruvate (Invitrogen), 50 units/ml penicillin and 50 ug/ml streptomycin (Invitrogen) at 37^{o}C, 95% air and 5% CO_2 in a humidified incubator. cFibro were maintained with DMEM containing 10% FBS, L-glutamine (Invitrogen), 4.5 g/L glucose, 100 units/ml penicillin, and 100

ug/ml streptomycin. All cells used for reprogramming were within 5 passages. Cells were passaged upon confluency by trypsinization. Derived ciPSCs were maintained on MEF feeder layers with iPSC medium containing Knockout DMEM (Invitrogen), 20% ES qualified FBS (Invitrogen), 2 mM L-Glutamine (Invitrogen), 1×10^{-4} M nonessential amino acids (Invitrogen), 1×10^{-4} M 2-mercaptoethanol (Invitrogen), 100 units/ml penicillin, 100 ug/ml streptomycin, 4 ng/ml human bFGF (Invitrogen), and 12.5 ng/ml human LIF (Millipore, Billeria, MA). cESCs were received as a gift from Dr. Beverly Torok Storb (Fred Hutchinson Cancer Research Center, Seattle, Washington) (1). cESCs were cultured under the same conditions as ciPSCs.

Production of lentiviral reprogramming vectors. 293FT cells were plated at ~80% confluence per 100 mm dish and transfected with 12 ug of each lentiviral vectors (Oct4, Sox2, Klf4, c-MYC) plus 8 ug of packaging plasmids and 4 ug of VSVG plasmids using Lipofectamine 2000 (Invitrogen, Carlsbad, CA) following manufacturer's instructions. The resulting supernatant was collected 48 hours after transfection, filtered through a 0.45 um pore-size cellulose acetate filter, and mixed with PEG-it Virus Concentration Solution (SystemBio, Mountain View, CA) overnight at 4^{o}C. Viruses were precipitated at 1500g the next day and resuspended with Opti-MEM medium (Invitrogen, Carlsbad, CA).

Immunofluorescence and alkaline phosphatase staining. Cells were fixed with 2% formaldehyde in PBS for 2 min, permeabilized with 0.5% tritonX-100 in PBS for 10 min, and blocked with 5% bovine serum albumin in PBS for one hour. Cells were then stained with appropriate primary antibodies and AlexaFluor conjugated secondary antibodies (Invitrogen, Carlsbad, CA). The primary antibodies for Oct3/4 (Santa Cruz, Santa Cruz, CA), Sox2

(Biolegend, San Diego, CA), Klf4 (Abcam, Cambridge, UK), c-MYC (Abcam), SSEA-3 (Millipore, Billeria, MA), SSEA-4 (Millipore), Tra-1-60 (Millipore), Tra-1-81 (Millipore), Nanog (Santa Cruz), Desmin (Sigma, St. Louis, MO), Sox17 (R&D Systems, Minneapolis, MN), and Tuj-1 (Covance, Princeton, NJ) were used in the staining (Supplemental Table 1). Alkaline phosphatase (AP) staining was performed using the Quantitative Alkaline Phosphatase ES Characterization Kit (Millipore Chemicon, Billeria, MA) following the manufacturer's instructions.

Quantitative-PCR. Total RNA and cDNA of each sample were prepared using the RNeasy Mini Plus Kit (Qiagen, Valencia, CA) and the QuantiTect Reverse Transcription Kit (Qiagen), respectively, following the manufacturer's instructions. Quantitative-PCR to measure mRNA expression levels was done with Taqman Gene Expression Assays (Applied Biosystems, Carlsbad, CA) using a SteponePlus Realtime-PCR System (Applied Biosystems) in the Protein and Nucleic Acid Facility at Stanford University School of Medicine. All primers are listed in Supplemental Table 2.

***In vitro* differentiation.** ciPSCs were treated with dispase (Invitrogen, Carlsbad, CA) and transferred to ultra-low attachment plates (Corning Life Sciences, Kennebunk, ME) in suspension culture for 8 days with DMEM/F12 (1:1) (Invitrogen) containing 20% knockout serum (Invitrogen), 4.5 g/L L-glutamine (Invitrogen), 1% nonessential amino acids (Invitrogen), 0.1 mM 2-mercaptoethanol (Invitrogen), 50 units/ml penicillin (Invitrogen), and 50 ug/ml streptomycin (Invitrogen). Embroid bodies (EBs) were then seeded in 0.25% gelatin-coated tissue culture dishes for another 8 days. Spontaneous differentiation of ciPSCs into cells of

ectoderm, mesoderm, and endoderm lineages was detected with appropriate markers by Q-PCR.

Teratoma formation. To form teratomas, ~2 million ciPS cells were harvested from culture dishes and injected subcutaneously to the dorsal flanks of adult SCID mice (n=6). After 8 weeks, tumors were dissected and fixed with 10% formaldehyde in PBS. Parrafin embedded tissue sections were then generated and stained with hematoxylin and eosin (H&E). Histological slides were interpreted by an expert pathologist (AJC).

Bioluminescence and micro positron emission tomography (microPET) imaging *in vitro* and *in vivo*. ciPSCs and cESCs which were stably transduced with a triple-fusion reporter gene carrying firefly luciferase, red fluorescent protein, and herpes simplex truncated thymidine kinase (LV-Fluc-RFP-HSVttk) driven by the ubiquitin promoter. Tumor growth was monitored noninvasively by BLI. Animals were injected with 250 mg/kg D-luciferin and imaged using a Xenogen IVIS Spectrum (Xenogen, Alameda, CA) as previously described (2). cESCs labeled with Fluc-RFP-HSVttk reporter gene were used as a positive control to monitor teratoma growth. microPET imaging was acquired using a R4 Concorde MicroPET system. Mice were injected with the reporter probe 9-[4-[^{18}F]fluoro-3-(hydroxymethyl)butyl]guanine ([^{18}F]-FHBG) (0.92±0.19 uCi) and imaged 60 to 75 minutes after injection. Images were reconstructed by filtered back-projection algorithm. For each imaging process, a set of serial microPET images was collected to assess the influx of the tracer for 90 min (18 frames, 5 min each). Regions of interest (ROIs) were drawn over the interested area. The ROI counts per milliliter per minute were converted to counts per gram per minute (assuming a tissue density of 1 g/mL) and divided by the injected dose to obtain an image ROI-derived [^{18}F]-FHBG percentage injected dose per

gram (% ID/g) as described previously (3). For *in vitro* imaging experiments, 1 ml of cells at the following four different concentrations (1×10^6, 2×10^6, 5×10^6, 10×10^6 cell/ml) were plated on 60 mm dishes. Cells were pre-incubated with 20 μCi/ml [^{18}F]-FHBG for 30 minutes before microPET image acquisition.

Microarray hybridization and data analysis. Total RNA samples were hybridized to Affymetrix GeneChip Canine Genome 2.0 Array, and then normalized and annotated by the Affymetrix® Expression Console™ software. A heatmap was generated for 164 genes that showed differences in expression greater than $\log_2$ ratio 6. The Pearson Correlation Coefficient was calculated for each pair of samples using the expression level of transcripts, which show standard deviation greater than 0.2 (17895 probes) among all samples. For hierarchical clustering, we used Pearson correlation for average linkage clustering. Scatter plots were generated for whole gene expression.

Intramyocardial delivery of autologous ciPSCs in canine models. Dogs were anesthetized with 5 mg/kg tiletamine/zolazepam (Webster, Sterling, Mass), tracheally intubated, and mechanically ventilated. Anesthesia was maintained with 2% isoflurane in 100% oxygen, and electrocardiogram, respiration rate, and intraventricular pressure were recorded. All dogs underwent a left lateral thoracotomy through the fourth and fifth intercostal spaces. The pericardium was opened and an octopus device was placed on the wall of the left ventricle at each injection site to facilitate injections into the heart by reducing the motion of the myocardium. After injection into the anterior myocardium, the chest wall was closed in layers and a pleural tube was placed into the left pleural cavity to drain the remaining free air.

Clinical PET-CT imaging of autologously transplanted ciPSCs. Imaging was performed with a clinical PET-CT scanner (Discovery LightSpeed Plus; GE Medical Systems, Waukesha, Wisconsin), with the animals in a supine position. After an initial scout view (30 mAs, 120 kV), a monenhanced four-detector CT scan of the heart was obtained with the following settings: section thickness of 5 mm, table feed of 38 mm per rotation, 0.8-second gantry rotation time; x-ray tube voltage of 120 kV, and tube current of 150 mA. Eight hours after intramyocardial injection of $1x10^8$ ciPSCs and 4 hours after intravenous administration of [^{18}F]-FHBG (mean, 536.5 MBq; range, 370–777 MBq), a 1-hour static PET scan was acquired. Transverse section reconstructions of the CT data sets were performed with a nominal section thickness of 5 mm at an interval of 4.25 mm. All PET images were reconstructed by using an iterative algorithm (ordered-subset expectation maximization, two iterative steps, 28 subsets), with CT-based attenuation correction applied. No cardiac gating or respiratory motion correction was performed.

Labeling of ciPSCs with iron particles. We labeled ciPSCs with Feridex IV-protamine sulfate (FE-Pro) as described previously (4). The commercially available superparamagnetic iron oxide (SPIO) suspension (Feridex IV; Berlex Laboratories, Inc, Wayne, NJ; http://berlex.bayerhealthcare.com/index.html) contains particles approximately 80–150 nm in size and has a total iron content of 11.2 mg/ml. We prepared preservative-free protamine sulfate (American Pharmaceuticals Partner Inc., Schaumburg, IL; http://www.appdrugs.com/) with a concentration of 10 mg/ ml using a fresh stock solution of 1 mg/ml and distilled water. SPIO at a concentration of 100 μg/ml was placed into a mixing tube containing serum-free culture medium. We added protamine sulfate (12 μg/ml) and mixed the entire suspension for 5–10 minutes. We added the final FE-Pro suspension to the existing medium and incubated

overnight. The final concentrations of Feridex IV and protamine sulfate were 50 and 6 μg/ml of medium, respectively. After overnight incubation, the ciPSCs were washed twice with PBS and harvested by treatment with collagenase IV and trypsin, respectively.

MR imaging of autologously transplanted ciPSCs. Imaging was performed on a Signa 3.0T Excite HD scanner (http://www.gehealthcare.com/euen/mri/index.html) with an 8-element phased array coil (GE Healthcare Systems, Milwaukee, Wisconsin). Dogs were intubated, anesthetized, and placed in the supine position for imaging. An electrocardiogram and respiratory gating system was used to acquire images. Briefly, a three-dimensional-plane localization was performed. Iron labeled cells were imaged in oblique planes using a gradient-recalled echo (GRE) sequence (repetition time 100 ms, echo time 10 ms, flip angle 30°, slice thickness 1 mm, slice gap 0 mm). Multiple contiguous slices were acquired for complete coverage of the dog heart.

Ex vivo **imaging of dog heart by microPET.** Following PET-CT imaging, animals were sacrificed by intravenous administration of saturated potassium chloride. Hearts were explanted and sectioned in a short-axis plane for *ex-vivo* imaging by microPET. A 4 minute static image was acquired for each section after which the hearts were fixed for histology.

Histology of dog heart. Animal hearts were excised, rinsed, fixed in 10% neutral buffered formalin overnight, and sectioned in transverse slices. Transverse slices from the level of injection were verified by gross examination, and H&E staining was performed by means of paraffin embedding.

Differentiation of ciPSCs into canine endothelial cells (ciPSC-ECs). Generation of ciPSC-ECs was based on previous endothelial cell differentiation protocols using human ESCs and iPSCs (5). Briefly, ciPSCs were cultured in ultra low attachment dishes using EB differentiation medium consisting of Knock out DMEM (KDMEM; Invitrogen), 20% ES qualified FBS (Invitrogen), 2 mM L-Glutamine, 1×10^{-4} M nonessential amino acids (Invitrogen), 1×10^{-4} M 2-mercaptoethanol, and 1X pen/strep (Invitrogen). After two days suspension culture, EBs were collected and transferred to 0.2% gelatin coated dishes using medium containing KDMEM, 20% FBS, 2 mM L-Glutamine, 1×10^{-4} M nonessential amino acids, 1×10^{-4} M 2-mercaptoethanol, 1x pen/strep, 200 ng/ml VEGF (R&D Systems, Minneapolis, MN), 20 ng/ml IGF (R&D), 50 ug/ml Ascorbic acid (R&D), and 1 ug/ml Hydrocortisone (R&D). Medium was changed every other day. After 16 days culture, cells were passaged using 0.25% trypsin and replated on collagen IV coated dishes using endothelial cell culture medium containing EGM-2 (Lonza, MD). For DiI-ac-LDL uptake, iPSC-EC were incubated with 10ug/ml of DiI-AC-LDL (Molecular Probes, OR) at 37 for 6 hours. After washing with PBS twice, cells were fixed and counterstained with DAPI as described. The formation of endothelial tubes was assessed by seeding cells in 24-well plates coated with Matrigel and incubating them at 37°C for 12 hours as described.

Delivery of ciPSC-ECs in a murine model of hindlimb ischemia. SCID Beige mice (Charles Rivers Laboratories, MA) were anesthetized with isoflurane (2-3%) after which unilateral hindlimb ischemia was induced by ligating the femoral artery. Briefly, skin on the right leg of the mouse was dissected from the knee towards the medial thigh. After separation of the femoral artery and vein, a segment of the femoral artery was tied with a 7-0 suture and

subsequently transected with spring scissors (6,7). To test the therapeutic potential of ciPSC-ECs, $1x10^6$ cells stably expressing Fluc-RFP-HSVttk were delivered by intra-muscular injection into the region of ischemia (n=5). Control animals received PBS (n=5).

Laser Doppler of hindlimb perfusion. Blood perfusion of ligated and control hindlimbs was assessed using a PeriScan PIM3 laser Doppler system (Perimed AB, Sweden) as previously described (6). Animals were placed on a 37°C heatpad, and hindlimb blood flow was measured on days 0, 7, and 14. Perfusion was quantified as mean pixel value within the entire hindlimb and the relative changes in hindlimb blood flow were expressed as the pixel ratio of the ischemic leg over the nonischemic leg.

SUPPLEMENTAL FIGURE LEGEND

Supplemental Figure 1. Pluripotency of ciPSCs derived from cASC and cFibro. ciPSCs derived from cASCs and cFibro both stained positive for standard markers of pluripotency. **(A)** DAPI staining of ciPSCs (ASC). **(B)** Oct-4 (green) and Tra-1-60 (red) co-staining of a ciPSC (ASC) colony. **(C)** ciPSCs (ASC) colonies stain positive for alkaline phosphastase (AKP). **(D)** DAPI staining of ciPSCs (Fibro) colony. **(E)** ciPSCs (Fibro) express Oct-4 and Tra-1-60 in an identical fashion to ciPSCs (ASC). **(F)** ciPSCs (Fibro) express AKP in an indistinguishable manner from c-ASC-iPSCs.

Supplemental Figure 2. Semi-quantative RT-PCR analysis of ciPSCs and cASCs. ciPSCs (ASC) were positive for expression of pluripotency genes Oct-4, Nanog, Sox2, Klf-4, Nanog, and c-Myc. Parental cASCs and embroid bodies differentiated from ciPSCs (ASC) did not express these pluripotency genes.

Supplemental Figure 3. Whole genome analysis of cASCs, ciPSCs (ASC), and cESCs. Scatter plots of whole genome expression show similarities between cESC and ciPSC transcriptional profiles and marked differences between cESCs/ciPSCs and cASCs. Principal component analysis for whole genome expression further verifies the similarities in cESC and ciPSC gene expression profiles as compared to cASCs.

Supplemental Figure 4. Microarray analysis of cASCs, ciPSCs (ASC), ciPSCs (Fibro), and cESCs. Microarray analysis identified 164 genes which showed significant differences in gene expression between cESCs and cASCs (log_2 ratio greater than 6). Expression of these genes was

compared in ciPSCs, cESCs, and cASCs. Specifically, 1 cell line of cASCs, 2 cell lines of ciPSCs derived from cASCs denoted as ciPSCs (ASC-1) and ciPSCs (ASC-2), 2 cell lines of ciPSCs derived from cFibro denoted as ciPSCs (Fibro-1) and ciPSCs (Fibro-2), and 2 cell lines of cESCs were compared. ciPSCs (Fibro), ciPSCs (ASC) and cESCs were found to have similar expression profiles for these genes in contrast to cASCs.

Supplemental Figure 5. Quantitative PCR of ciPSC (ASC)-derived EBs. Embroid bodies (EBs) derived from ciPSCs (ASC) were subjugated to Q-PCR analysis for an array of genes associated with differentiation. Specifically, these include FoxA2 (endoderm), TJF (ectoderm), AFP (endoderm), Gata4 (mesoderm), Gata6 (mesoderm), MLC (mesoderm), Nkx (mesoderm), and Gbx (ectoderm). Differentiated cells derived from c-ASC-iPSCs were found to express genes from all three germ layers while ciPSCs (ASC) and cESCs did not express these genes.

Supplemental Figure 6. Quantitative PCR of ciPSC (Fibro)-derived EBs. EBs derived from ciPSCs (Fibro) were subjugated to Q-PCR analysis for an array of genes associated with differentiation. Specifically, these include FoxA2 (endoderm), TJF (ectoderm), AFP (endoderm), Gata4 (mesoderm), Gata6 (mesoderm), MLC (mesoderm), Nkx (mesoderm), and Gbx (ectoderm). Differentiated cells derived from c-fibro-iPSCs were found to express genes from all three germ layers while ciPSCs (Fibro) and cESCs did not express these genes.

Supplemental Figure 7. Histology of dog heart. Histological sections of dog hearts were stained by hematoxylin and eosin (H&E). **(A)** Myocardial tissue remote to the site of cell injection is healthy with no cell death (20X). **(B)** Myocardial tissue at site of injection has

minimal cell death and little evidence of inflammatory infiltrate due to autologous nature of transplantation (20x). **(C)** Magnified view of remote myocardium (40x). **(D)** Magnified view of injection site (40x).

Supplemental Figure 8. Generation of ciPSC-ECs and delivery into murine model of hindlimb ischemia. (A) ciPSC-ECs stained positive for CD31, demonstrated DiI-ac-LDL uptake, and formed tubules when cultured on Matrigel *in vitro*. **(B)** A representative animal post hindlimb ligation injected with $1x10^6$ ciPSC-ECs demonstrates significant bioluminescence activity at day 2, which decreases progressively over the following 2 weeks. **(C)** Quantitative analysis of BLI signal in animals transplanted with ciPSC-ECs. Signal activity is expressed as photons/sec/cm^2/sr. **(D)** Laser Doppler of blood perfusion in ischemic legs of mice demonstrates improved revascularization in animals receiving ciPSC-ECs as compared to animals receiving saline. **(E)** Quantification of blood flow reveals improved reperfusion in hindlimbs of mice receiving ciPSC-ECs compared to PBS control.

SUPPLEMENTAL VIDEO LEGEND

Supplemental Video 1: Three dimensional PET-CT reconstruction of the thorax and upper abdomen in the same dog reveals high [^{18}F]-FHBG uptake in the myocardium corresponding to the location of injected ciPSCs. There is high signal in the liver due to natural route of [^{18}F]-FHBG excretion via biliary and hepatic routes as has been shown in human dendritic cell imaging study (lower left) (8).

Supplemental Table 1: Primary antibody information

Antibody	Company	Catalog #	Dilution
OCT4	Santa Cruz	SC-9081	1:100
NANOG	Santa Cruz	sc-33759	1:100
SOX2	Stem Cell Tech	1438	1:50
SSEA-4	Chemicon	MAB4304	1:50
Tra-1-61	Abcam	ab16288	1:50
Sox-17	B&D	AB2132	1:200
Nkx2.5	Abcam	ab22611	1:200
NFH	Antibodies	ABIN141440	1:50

Supplemental Table 2: Primer sequences

Primers	Sequences (5'-3')
Oct-4	TCGTGAAGCCGGACAAGGAGAAG
	AGGAACATGTTCTCCAGGTTGCCT
Nanog	CCTGCATCCTTGCCAATGTC
	TCCGGGCTGTCCTGAGTAAG
Sox-2	AACCCCAAGATGCACAACTC
	CGGGGCCGGTATTTATAATC
Klf-4	CCATGGGCCAAACTACCCAC
	TGGGGTCAACACCATTCCGT
Cmyc	GCCAAAAGGTCGGAATCGGGG
	CGCAGCACGTCTTTTTCTGACAC
AFP	TGCCAGGCTCAGGGTGTAG
	TAAACTCCCAAAGCAGCACGA
GATA4	AACGGAAGCCCAAGAACCTT
	GCCACATTGCTGGAGTTGCT
GATA6	CATTTGGAGGAAACCGTGAA
	CCAGCAAATGCAGATTCCTT
MLC	CCACTCTGGGTGAGAGGCTA
	GGGCTGCCGTAGGATTCTC
Nkx	CCAAGGACCCTCGAGCTGA
	CGACAGATACCGCTGCTGCT
Gbx	TGCAGGCGTCGCTCGTAG
	TCCGAGCTGTAGTCCAGATCA
GAPDH	TATCAGTTGTGGATCTGACCTG
	GCGTCGAAGGTGGAAGAGT

SUPPLEMENTAL REFERENCES

1. Vaags, A. K., Rosic-Kablar, S., Gartley, C. J., Zheng, Y. Z., Chesney, A., Villagomez, D. A., Kruth, S. A., and Hough, M. R. (2009) *Stem Cells* **27**(2), 329-340
2. Cao, F., Li, Z., Lee, A., Liu, Z., Chen, K., Wang, H., Cai, W., Chen, X., and Wu, J. C. (2009) *Cancer Res* **69**(7), 2709-2713
3. Cao, F., Lin, S., Xie, X., Ray, P., Patel, M., Zhang, X., Drukker, M., Dylla, S. J., Connolly, A. J., Chen, X., Weissman, I. L., Gambhir, S. S., and Wu, J. C. (2006) *Circulation* **113**(7), 1005-1014
4. Li, Z., Suzuki, Y., Huang, M., Cao, F., Xie, X., Connolly, A. J., Yang, P. C., and Wu, J. C. (2008) *Stem Cells* **26**(4), 864-873
5. Li, Z., Hu, S., Ghosh, Z., Han, Z., and Wu, J. C. (2011) *Stem Cells Dev.* Epub ahead of print
6. Niiyama, H., Huang, N. F., Rollins, M. D., and Cooke, J. P. (2009) *J Vis Exp* (23)
7. Huang, N. F., Niiyama, H., De, A., Gambhir, S. S., and Cooke, J. P. (2009) *J Vis Exp* (23)
8. Yaghoubi, S. S., Jensen, M. C., Satyamurthy, N., Budhiraja, S., Paik, D., Czernin, J., and Gambhir, S. S. (2009) *Nat Clin Pract Oncol* **6**(1), 53-58

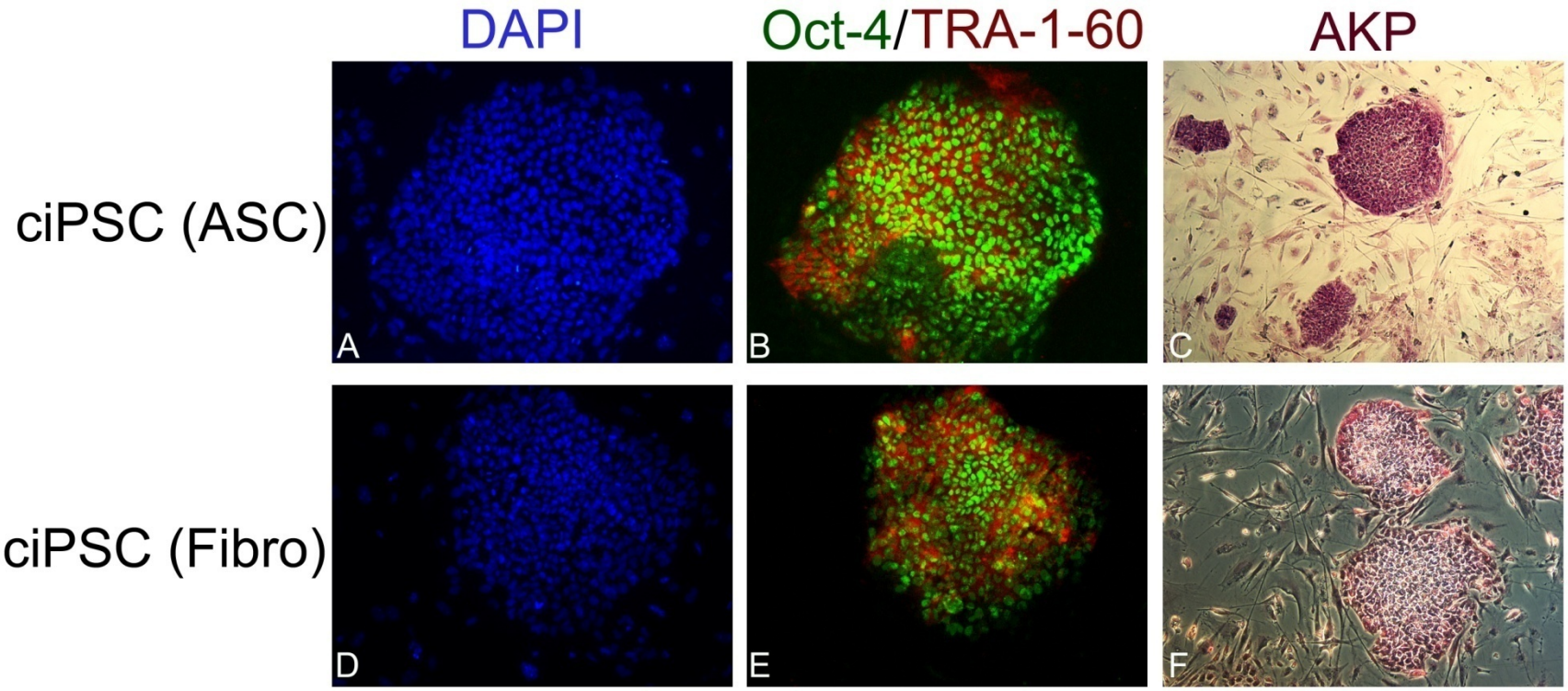

Supplemental Figure 1

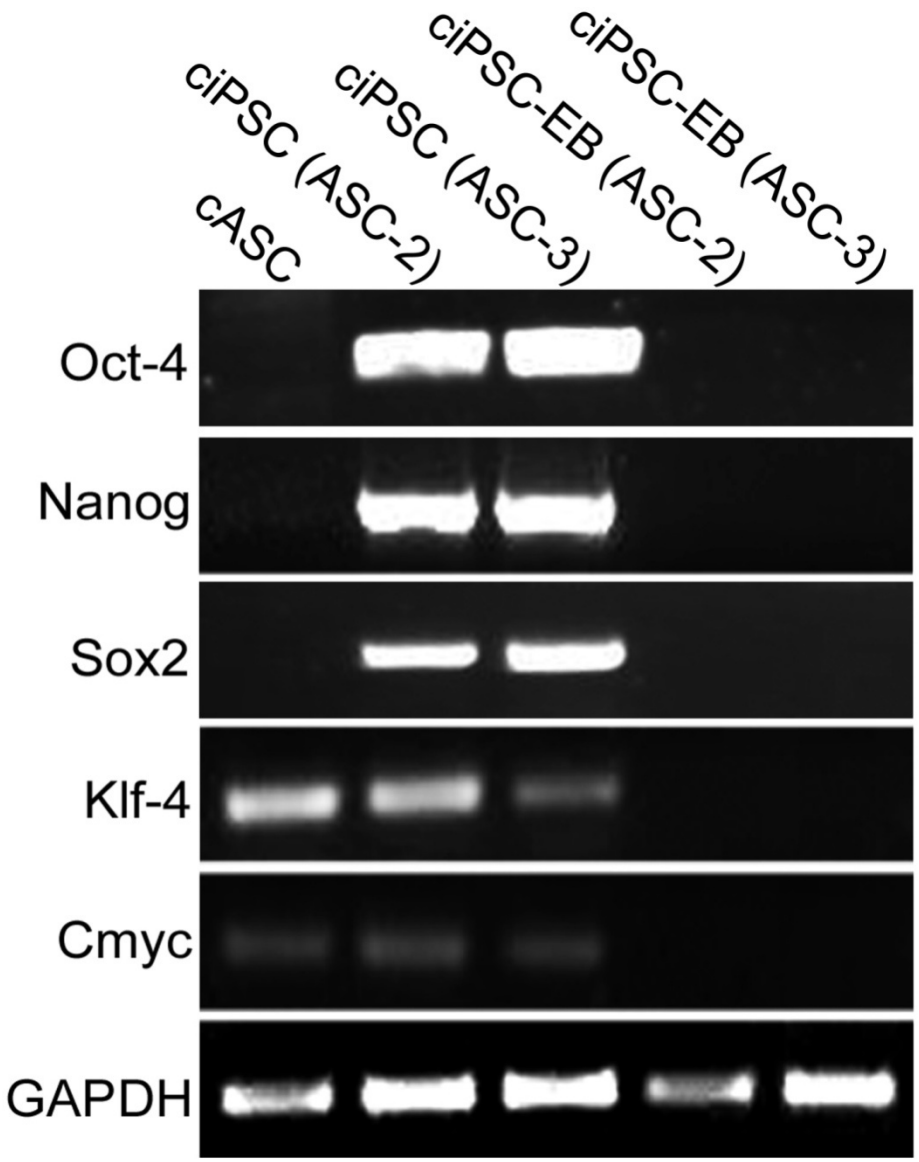

Supplemental Figure 2

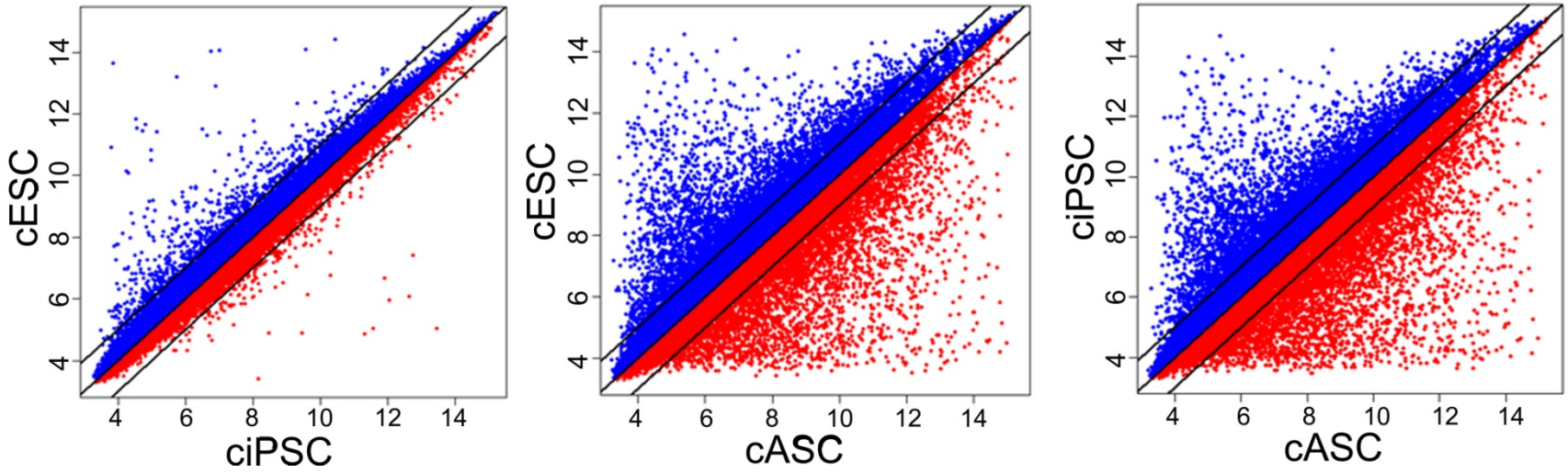

Supplemental Figure 3

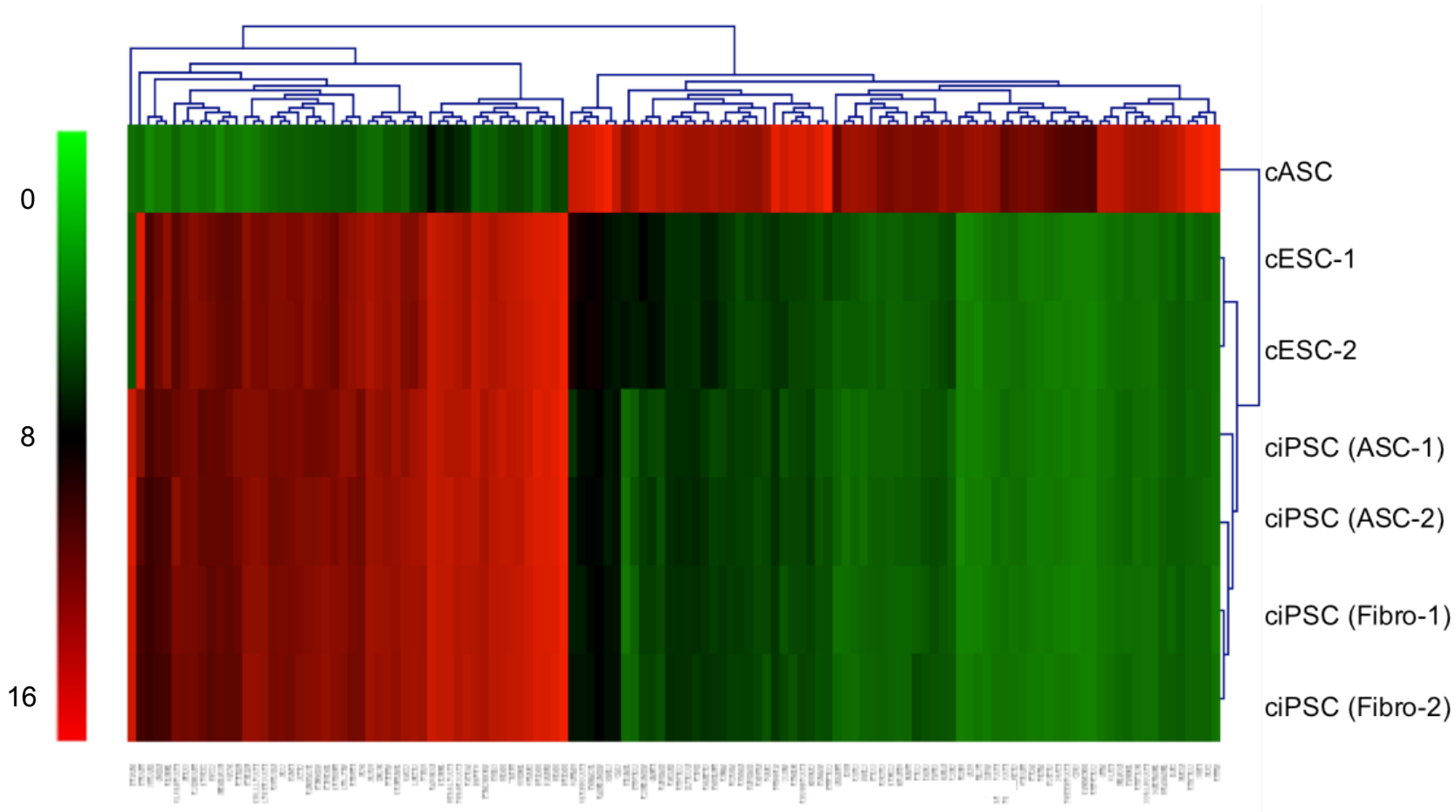

Supplemental Figure 4

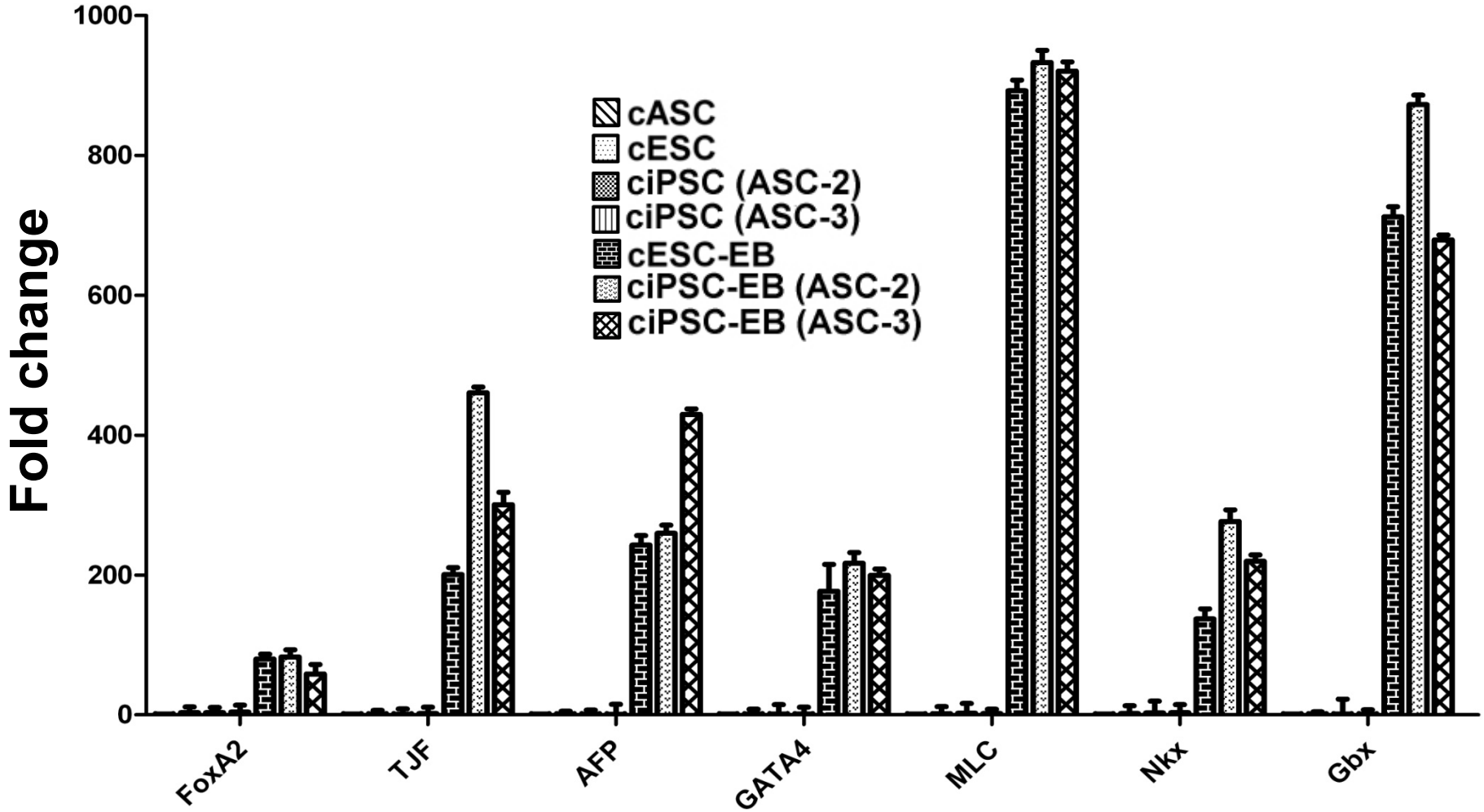

Supplemental Figure 5

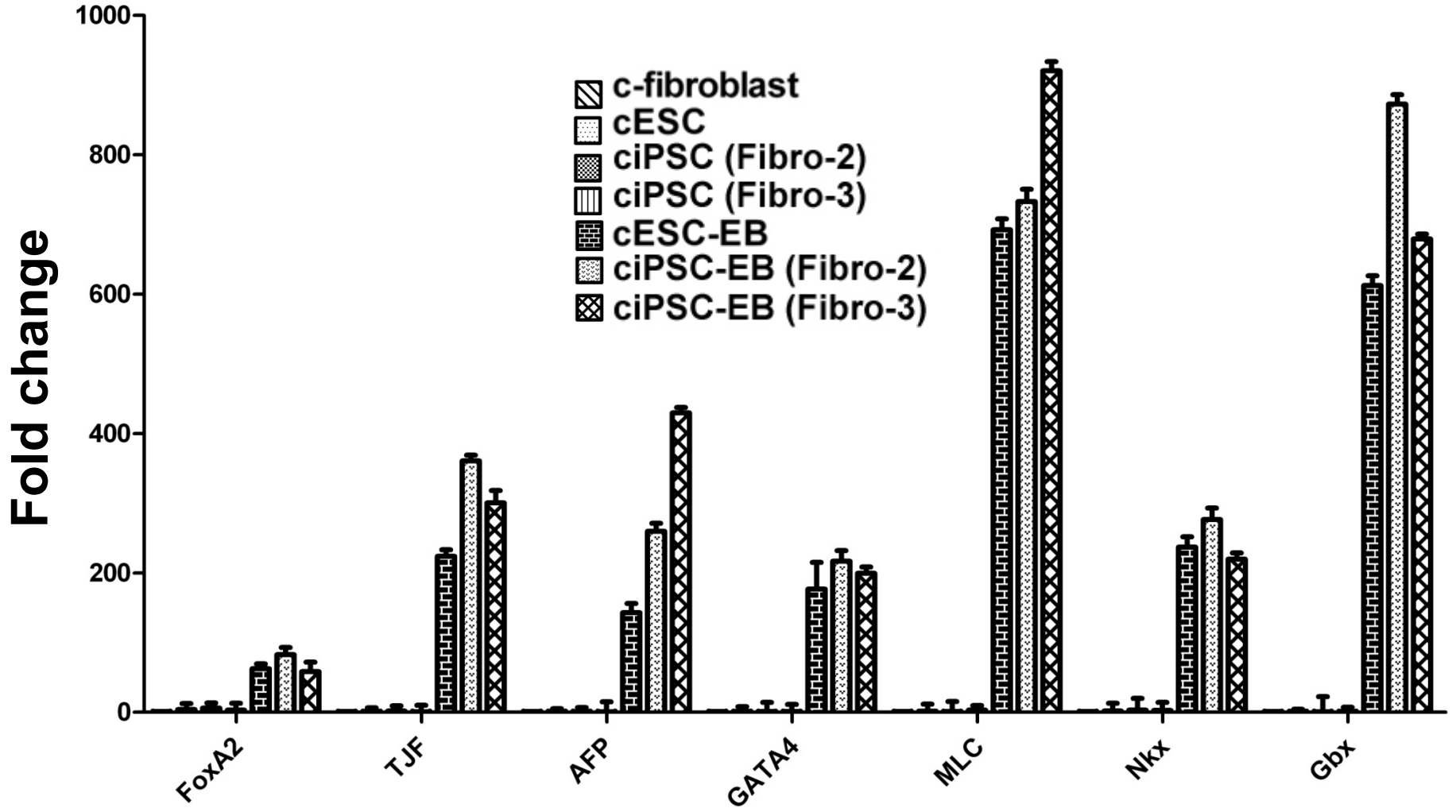

Supplemental Figure 6

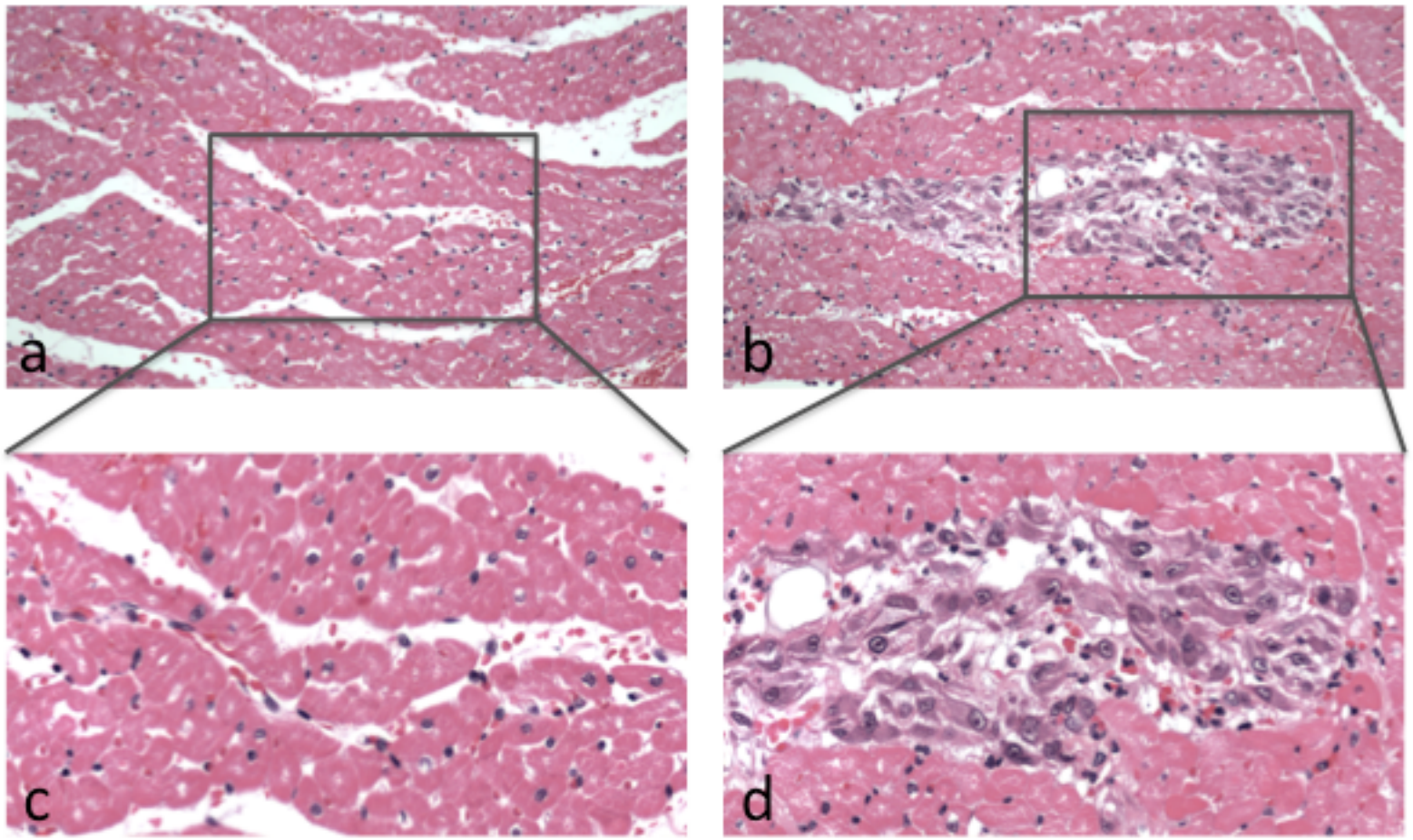

Supplemental Figure 7

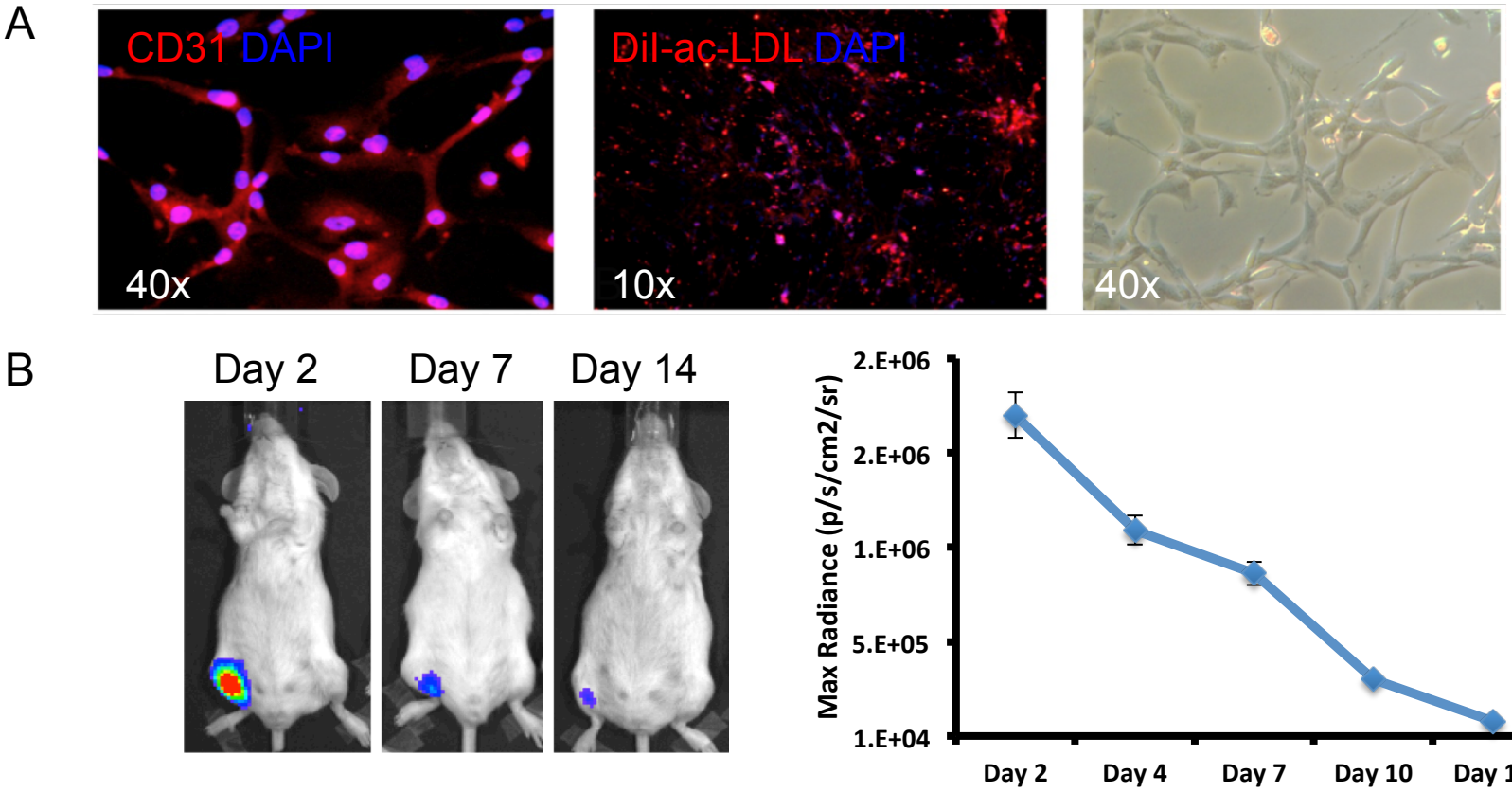

Supplemental Figure 8